

## A Photochemical Metallocene Route to Anionic Eneidyne: Synthesis, Solid-State Structures, and *ab Initio* Computations on Cyclopentadienoidenediynes

Joseph M. O'Connor,<sup>\*,†</sup> Kim K. Baldrige,<sup>\*,‡</sup> Betsy L. Rodgers,<sup>†</sup> Marissa Aubrey,<sup>†</sup> Ryan L. Holland,<sup>†</sup> W. Scott Kassel,<sup>†</sup> and Arnold L. Rheingold<sup>\*,†</sup>

Department of Chemistry, University of California, San Diego, La Jolla, California 92093, and Institute of Organic Chemistry, University of Zürich, Winterthurerstrasse 190, CH-8057 Zürich, Switzerland

Received June 12, 2010; E-mail: jmoconnor@ucsd.edu; kimb@oci.uzh.ch; arheingold@ucsd.edu

**Abstract:** The first demonstration of photochemical enediyne liberation from a metal complex has led to a new class of enediynes, the cyclopentadienoidenediynes, which are demonstrated to exist as air-stable solids with low ionization potentials and large dipole moments. NMR and IR spectroscopy, X-ray crystallography, and *ab initio* computations enable a comparison with the ubiquitous benzoenediynes.

Conjugated enediynes (**1**; Figure 1) are widely utilized as precursors to parabenzyne intermediates<sup>1</sup> and as key components in carbon-rich materials, such as bowl-shaped fullerene fragments, conjugated polymers, and carbon allotropes.<sup>2</sup> In all of these, advances have been greatly facilitated by the design and synthesis of novel enediyne structures. A widely employed strategy for stabilization of enediynes toward spontaneous polymerization<sup>3</sup> involves incorporation of the ene function into an aromatic ring, as in the benzoenediynes (**2**). Here we report the first photochemical liberation of an enediyne from a metal complex to give a new class of enediynes, the cyclopentadienoidenediynes (**3**), in which the ene function is incorporated into a cyclopentadienide ring.

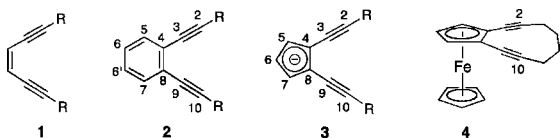
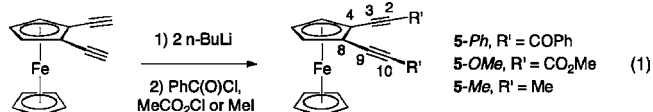


**Figure 1.** Acyclic enediynes (**1**), benzoenediynes (**2**), cyclopentadienoidenediynes (**3**), and iron enediynes (**4**). The numbering used in the text is also shown.

Despite the well-established photochemical stability of ferrocene derivatives in nonhalogenated solvents,<sup>4</sup> the long-standing observation that ferrocenes with conjugating substituents (e.g.,  $-\text{CO}_2\text{H}$ ,  $-\text{COR}$ ) may undergo photochemical ligand loss<sup>5</sup> led us to examine a metallocene route toward cyclopentadienoid analogues of benzoenediynes. The desired precursors **5-Ph** and **5-OMe** were readily prepared by sequential reaction of 1,2-diethynylferrocene (2.1 mmol, THF)<sup>6</sup> with *n*-BuLi (5.2 mmol) followed by quenching of the dianion with benzoyl chloride and methyl chloroformate, respectively, in slight excess (eq 1):

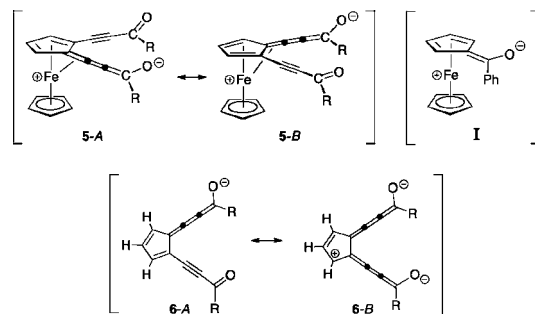


<sup>†</sup> University of California, San Diego.

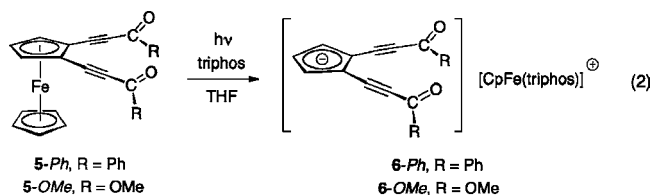
<sup>‡</sup> University of Zürich.

In this manner, **5-Ph** and **5-OMe** were prepared as red crystalline solids in 49 and 67% isolated yields. In the IR spectra (NaCl) of **5-Ph** and **5-OMe**, the carbonyl stretch is observed at 1633 and 1701  $\text{cm}^{-1}$ , respectively. For the series of diyne complexes ( $\eta^5\text{-C}_5\text{H}_5$ )Fe( $\eta^5\text{-C}_5\text{H}_3(\text{C}\equiv\text{CMe})_2$ ) (**5-Me**),<sup>7</sup> **5-OMe**, and **5-Ph**,  $\nu(\text{C}\equiv\text{C})$  decreases from 2235 to 2215 to 2190  $\text{cm}^{-1}$ , consistent with increasing delocalization as the alkyne substituent is varied along the series. A similar trend was observed in the <sup>1</sup>H NMR spectra (CDCl<sub>3</sub>), for which the hydrogen resonances of both cyclopentadienyl ligands are observed to shift progressively downfield as the alkyne substituent becomes more electron-withdrawing: **5-Me** ( $\delta$  4.22, s, 5H; 4.10, t, 1H; 4.53, t, 2H); **5-OMe** ( $\delta$  4.33, s, 5H; 4.48, t, 1H; 4.73, d, 2H); **5-Ph** ( $\delta$  4.40, s, 5H; 4.65, t, 1H; 4.93, d, 2H). In the solid-state structures of **5-Me**, **5-OMe**, and **5-Ph**, the iron–C3/C9 average distances are 3.130(5), 3.097(1), and 3.078(1) Å, respectively.<sup>8,9</sup> Thus, the spectroscopic and crystallographic data are consistent with contributions from cumulene resonance forms **5-A** and **5-B** (Scheme 1). These resonance structures are similar to the metal–ligand charge-transfer (MLCT) excited state **I** that has been proposed for the photochemical loss of the substituted cyclopentadienyl ligand in benzoylferrocene.<sup>5a</sup>

**Scheme 1.** Resonance Contributors for **5** and **6** and the Proposed<sup>5a</sup> Excited State **I** for Ligand Loss upon Photolysis of CpFe[C<sub>5</sub>H<sub>3</sub>(COR)<sub>2</sub>]



Unlike cyclic iron–enediyne complexes **4** (Figure 1) and **5-Me**, both **5-OMe** and **5-Ph** are light-sensitive compounds. Initial attempts at generating a cyclopentadienoidenediyne by photolysis of **5-Ph** in THF solution led to the formation of an intractable brown precipitate, ferrocene, and free cyclopentadiene, with no clear evidence of the desired product. However, when a THF-*d*<sub>8</sub> solution containing **5-Ph** (0.045 mmol) and 1 equiv of tris(diphenylphosphinomethyl)ethane (triphos) was irradiated with a medium-pressure Hanovia lamp (2 h), nearly quantitative conversion to **6-Ph** was observed by <sup>1</sup>H NMR spectroscopy (eq 2):



A preparative scale reaction led to the isolation of **6-Ph** as a dark-red (almost black) crystalline solid. In a similar fashion, compound **6-OMe** was isolated as dark-brown air-stable crystals by irradiation of **5-OMe**.<sup>10</sup>

In the <sup>1</sup>H NMR spectra (THF-*d*<sub>8</sub>) of **6-Ph** and **6-OMe**, the substituted cyclopentadienyl ring hydrogens resonate 1.2–1.7 ppm downfield of those for the iron precursors, with the C5/C7 hydrogens significantly more deshielded relative to the C6 hydrogen: **6-Ph** ( $\delta$  5.84, t,  $J$  = 3 Hz, 1H; 6.43, d,  $J$  = 3.5 Hz, 2H); **6-OMe** ( $\delta$  5.87, m, 1H; 6.45, d,  $J$  = 2.5 Hz, 2H). The C<sub>5</sub>H<sub>5</sub> hydrogens of the iron cation in **6-Ph** ( $\delta$  4.95) exhibit a different chemical shift than those in **6-OMe** ( $\delta$  4.84), suggesting that the anion and cation are not completely solvent-separated in THF solution. The addition of D<sub>2</sub>O to an acetonitrile-*d*<sub>3</sub> solution of **6-OMe** results in the very slow incorporation of deuterium into the three ring-hydrogen positions of the substituted five-membered ring. In the IR spectrum (KBr, thin film) of **6-OMe**, bands are observed at 2124 (C≡C), 2155 (C≡C), and 1671 (C=O) cm<sup>-1</sup>. These can be compared with the values of 2215 (C≡C) and 1701 (C=O) cm<sup>-1</sup> for **5-OMe** (KBr, thin film). Taken together, the <sup>1</sup>H NMR and IR data indicate significant contributions from cumulene resonance forms **6-A** and dicumulene forms **6-B** (Scheme 1).

The solid-state structures of **6-OMe** and **6-Ph** were determined by X-ray crystallographic analyses (Figure 2, Table 1).<sup>11</sup> There are two independent molecules within the unit cell of **6-Ph**, indicated here as **6-Ph-A** and **6-Ph-B**. Within experimental uncertainty, the C4–C8, C2–C3, and C9–C10 bond distances of the enediyne framework are the same in the three structures and similar to the related values in the solid-state structures of iron precursors **5-OMe** and **5-Ph**. The C4–C8 “ene” distances of 1.439(5)–1.457(4) Å in **6** are significantly longer than the distance of 1.346(3) Å in the one reported example of a structurally characterized cyclopentene-1,2-diyne.<sup>12</sup> The cyclopentadienido ring in all three structures is essentially planar, with the largest deviation of the sp carbons from the mean plane occurring at C10 in **6-OMe** (0.16 Å) and C2 in **6-Ph-B** (0.31 Å). The most significant bond angle distortions are in the C9–C10–C11 angles, which range from 168.0° in **6-Ph-A** to 171.2° in **6-OMe**.<sup>13</sup> The significant bending at C10, along with minor bending at C9 (174.1–178.3°), and large displacements of the O2 carbonyl oxygen atom from the ring plane (0.48–0.68 Å) result in significant curvature along C8–C9–C10–C11–O2. In the crystal lattice of **6-OMe**, the concave face of the curve is presented toward the triphos ligand of the cation, whereas in the lattice of **6-Ph-A**, the convex side of the curve is presented toward the triphos ligand. The C3–C4–C8–C9 torsion angles in **6-Ph-A** and **6-Ph-B** are 0.81(52) and –6.70(55)°, respectively, and the closest nonbonded distances between benzoyl groups are the C14A···O2A distance of 3.308(4) Å in **6-Ph-A** and the corresponding distance of 3.085(5) Å in **6-Ph-B**. The O2A···H14A distance of 2.63 Å in **6-Ph-A** is 0.27 Å shorter than the O2B···H14B distance in **6-Ph-B**.

Of particular interest for enediyne structure–activity relationships is the so-called critical distance (or [*cd*] distance), corresponding to C2···C10 in **6**, which has been correlated with the ease of Bergman cycloaromatization.<sup>1b,c</sup> The C2···C10 distance of 4.565 Å in **6-OMe** is significantly longer than that in **6-Ph-A** (4.449 Å),

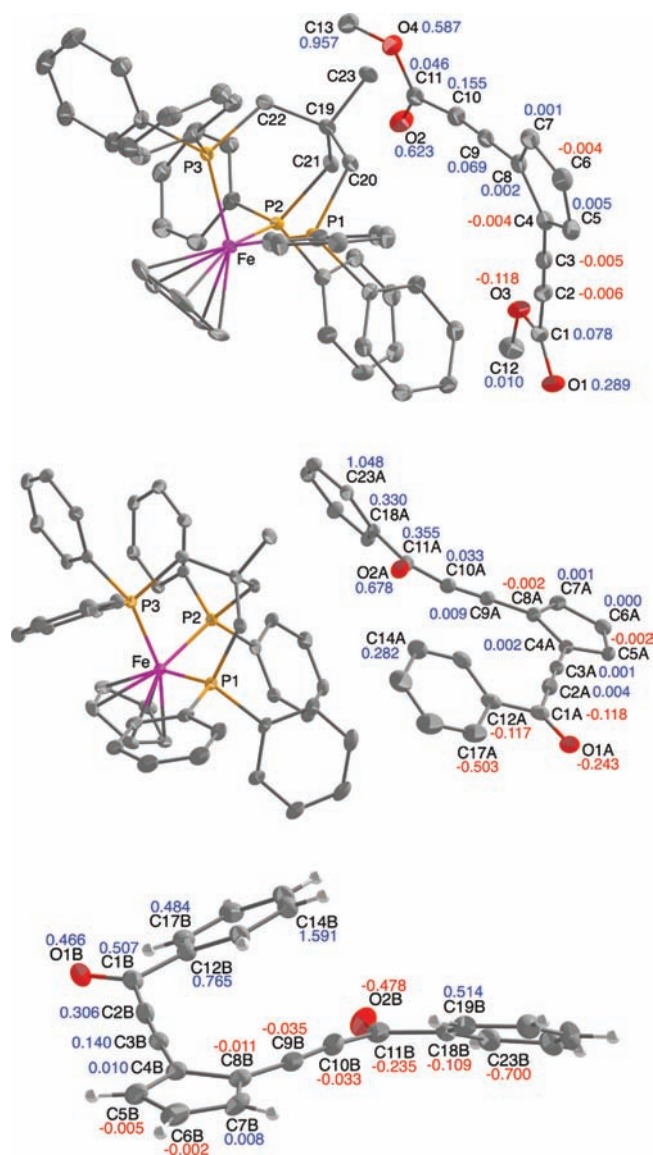


**Figure 2.** ORTEP drawings of (top) **6-OMe** and (center) **6-Ph-A**, in which hydrogen atoms have been omitted for clarity, and (bottom) the anion of **6-Ph-B**. Red and blue numbers indicate atom displacements from the C4–C5–C6–C7–C8 mean plane ( $\leq 0.003$  Å).

**Table 1.** Bond Lengths (Å) and Angles (deg) for the Anions in **6-Ph**, **6-OMe**, **6-OMe-calc**, and **7-calc**

	<b>6-Ph-A</b>	<b>6-Ph-B</b>	<b>6-OMe</b>	<b>6-OMe-calc</b>	<b>7-calc</b>
C2···C10	4.449(4)	4.256(5)	4.565(4)	4.608	4.137
C1–C2	1.426(5)	1.417(5)	1.439(4)	1.419	1.449
C2–C3	1.215(5)	1.220(5)	1.202(4)	1.214	1.201
C3–C4	1.392(4)	1.394(5)	1.411(4)	1.369	1.426
C4–C8	1.457(4)	1.439(5)	1.438(4)	1.440	1.409
C8–C9	1.414(4)	1.406(6)	1.400(4)	1.396	1.426
C9–C10	1.206(4)	1.221(6)	1.206(4)	1.214	1.201
C10–C11	1.439(4)	1.436(5)	1.423(4)	1.419	1.450
C1–C2–C3	175.0(4)	176.8(3)	176.5(3)	178.28	177.57
C2–C3–C4	178.4(3)	177.0(3)	179.8(3)	178.97	179.09
C8–C9–C10	176.3(3)	174.1(4)	178.3(3)	178.97	179.09
C9–C10–C11	168.0(3)	171.2(4)	171.2(3)	178.26	177.57

which is in turn longer than the 4.256 Å distance in **6-Ph-B**. These values can be compared with the distances of 3.442(12) Å in the 10-membered ring enediyne **4**<sup>7</sup> and 4.535(6) and 4.587(6) Å in the two independent molecules in the unit cell of **6-Me**. The large range of [*cd*] distances in the cyclopentadienidoenediyne anions is the

result of crystal packing forces and is an indication of the remarkable flexibility of the enediyne framework.

M06-2X/TZVP density functional theory (DFT) computational studies were undertaken to elucidate the fundamental structural and electronic differences between cyclopentadienoidenediynes and benzoenediynes, as represented by the structures **6-OMe-calc** and **7-calc** (Figures 3 and 4, Table 1). The validity of the computational results is supported by the remarkably close agreement between the crystallographic and computational data for **6-OMe** and anion **6-OMe-calc**. The largest structural differences between **6-OMe** and **6-OMe-calc** are the 0.045 Å difference in the [cd] distance and the conformation about the C10–C11 bond, for which the carbonyl oxygen (O2) is oriented endo (pointing toward the other alkyne) in the solid-state structure. The exo–exo gas-phase structure is calculated to be the lowest-energy conformer by 0.5 kcal/mol. Both structural differences are attributed to crystal lattice packing forces. The C4–C8, C2–C3, and C9–C10 distances as well as the [cd] distance are longer in cyclopentadienoidenediyne **6-OMe-calc** than in **7-calc**, leading to the prediction of a significantly higher activation energy for Bergman cycloaromatization in the former. We have observed only decomposition to uncharacterized products upon heating **6-OMe** in THF at 150°. It is anticipated that incorporation of the enediyne into a 10-membered ring (as in **4**) will lead to accelerated cycloaromatization rates in the metal-free system relative to strained-ring benzoenediynes as a result of significant strain-induced destabilization of the cyclopentadienoidenediyne ground-state structures. The  $\Delta$ SCF (Koopmans') theory gas-phase ionization potentials for **6-OMe-calc** and **7-calc** are 3.70 (3.05) and 9.10 (8.37) eV, respectively.<sup>14</sup> These can be compared with the values of 2.03 (1.44) and 9.53 (8.41) eV for cyclopentadienide and benzene, respectively. The dipole moments are 6.4 D for **6-OMe-calc** and 0.44 D for **7-calc**. A perspective of the frontier orbital energies (in eV) for **6-OMe-calc** is shown in Figure 4.

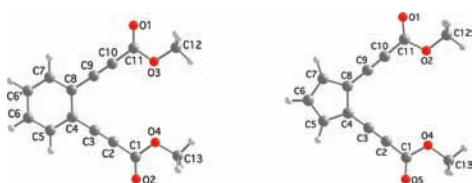


Figure 3. DFT structures of (left) **7-calc** and (right) **6-OMe-calc**.

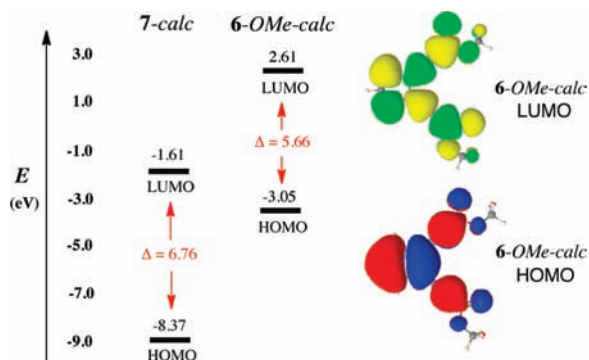


Figure 4. Frontier orbitals for (left) **7-calc** and (right) **6-OMe-calc** [MP2/DZ(2d,p) for **7-calc**:  $-9.09, 0.87$  eV;  $\Delta = 9.96$  eV. For **6-OMe-calc**:  $-3.73, 5.29$  eV;  $\Delta = 9.02$  eV.]

The reactions reported herein represent the first examples of photochemical enediyne liberation from a metal as well as the formation of a new class of enediynes, the cyclopentadienoidenediynes. We believe that photochemical dissociation of enediyne ligands will prove to be general with respect to other types of organometallic enediyne complexes (dienes, alkynes, etc.). Efforts are underway to prepare photoactive strained-ring enediynes that will spontaneously cycloaromatize upon enediyne dissociation from the metal.

**Acknowledgment.** Financial support by the National Science Foundation (CHE-0518707, CHE-0911765, and instrumentation grant CHE-9709183) is gratefully acknowledged. M.A. acknowledges the award of a Kamen/Kaplan Fellowship. K.K.B. acknowledges the Swiss National Science Foundation for support of this work.

**Supporting Information Available:** Experimental details for all new compounds, computational details for **6-OMe-calc** and **7-calc**, and crystallographic data for **5-Ph**, **5-OMe**, **5-Me**, **6-Ph**, and **6-OMe** (CIF). This material is available free of charge via the Internet at <http://pubs.acs.org>.

## References

- (1) (a) Perrin, C. L.; Rodgers, B. L.; O'Connor, J. M. *J. Am. Chem. Soc.* **2007**, *129*, 4795. (b) Rawat, D. S.; Zaleski, J. M. *Synlett* **2004**, 393. (c) Smith, A. L.; Nicolaou, K. C. *J. Med. Chem.* **1996**, *39*, 2103.
- (2) (a) Dosa, P. I.; Gu, Z.; Hager, D.; Karney, W. L.; Vollhardt, K. P. C. *Chem. Commun.* **2009**, 1967. (b) Wu, Y.-T.; Bandera, D.; Maag, R.; Linden, A.; Baldrige, K. K.; Siegel, J. S. *J. Am. Chem. Soc.* **2008**, *130*, 10729. (c) Hickenboth, C. R.; Rule, J. D.; Moore, J. S. *Tetrahedron* **2008**, *64*, 8435. (d) Spittler, E. L.; Johnson, C. A., II; Haley, M. M. *Chem. Rev.* **2006**, *106*, 5344. (e) Nielsen, M. B.; Diederich, F. *Chem. Rev.* **2005**, *105*, 1837.
- (3) For example, in neat solutions, **1** (R = CO<sub>2</sub>Et) polymerizes within minutes, whereas **2** (R = CO<sub>2</sub>Et) is thermally stable at ambient temperatures. See: König, B.; Pitsch, W.; Klein, M.; Vasold, R.; Prall, M.; Schreiner, P. R. *J. Org. Chem.* **2001**, *66*, 1742.
- (4) (a) Ornelas, C.; Méry, D.; Cloutet, E.; Aranzas, J. R.; Astruc, D. *J. Am. Chem. Soc.* **2008**, *130*, 1495. (b) Diallo, A. K.; Ruiz, J.; Astruc, D. *Inorg. Chem.* **2010**, *49*, 1913. (c) Stepnicka, P. *Ferrocenes: Ligands, Materials and Biomolecules*; Wiley: Chichester, England, 2008. (d) Barlow, S.; Henling, L. M.; Day, M. W.; Schaefer, W. P.; Green, J. C.; Hascall, T.; Marder, S. R. *J. Am. Chem. Soc.* **2002**, *124*, 6285.
- (5) (a) Yamaguchi, Y.; Ding, W.; Sanderson, C. T.; Borden, M. L.; Morgan, M. J.; Kutal, C. *Coord. Chem. Rev.* **2007**, *251*, 515. (b) Che, D. J.; Li, G.; Du, B. S.; Zhang, Z.; Li, Y. H. *Inorg. Chim. Acta* **1997**, *261*, 121. (c) Nesmeyanov, A. N.; Sazonova, V. A.; Romanenko, V. I. *Dokl. Akad. Nauk SSSR* **1963**, *152*, 1358.
- (6) Bunz, U. H. F. *J. Organomet. Chem.* **1995**, *494*, C8.
- (7) Baldrige, K. K.; Donovan-Merkert, B. T.; O'Connor, J. M.; Lee, L. I.; Closson, A.; Fandrick, D.; Tran, T.; Bunker, K. D.; Fouzi, M.; Gantzel, P. *Org. Biomol. Chem.* **2003**, *1*, 763.
- (8) Crystallographic details are provided in the Supporting Information.
- (9) In the solid-state structure of CpFe(C<sub>5</sub>H<sub>5</sub>C≡CCOPh), the Fe...C3 distance is 3.067 Å, which is consistent with a larger contribution from a cumulene resonance contributor than in the case of **5-Ph**. See: Arellano, I.; Sharma, P.; Arias, J. L.; Toscano, A.; Cabrera, A.; Rosas, N. J. *Mol. Catal. A: Chem.* **2007**, *266*, 294.
- (10) Sunlight also induces the reactions of triphos with both **5-OMe** and **5-Ph** to give nearly quantitative yields of **6-OMe** and **6-Ph**. In a control experiment, it was found that there is no reaction in the absence of light.
- (11) In the solid state, the anions in complexes **6** are well-separated from the metal [unlike those in most cyclopentadienide complexes, such as Na(TMEDA)C<sub>5</sub>H<sub>5</sub>] and thus represent rare examples of "η<sup>0</sup>"-cyclopentadienide anion. See: Casey, C. P.; O'Connor, J. M.; Haller, K. J. *J. Am. Chem. Soc.* **1985**, *107*, 1241, and references therein.
- (12) Kosinski, C.; Hirsch, A.; Heinemann, F. W.; Hampel, F. *Eur. J. Org. Chem.* **2001**, 3879.
- (13) A search of the Cambridge Structural Database indicated that the C9–C10–C11 angle of 168° in **6-Ph** is at the low end of the range for acyclic alkynes.
- (14) In chloroform solution, **6-OMe** undergoes decomposition over the course of days to give uncharacterized paramagnetic products.

JA105149K